

Observation of shell effects in nanowires for the noble metals copper, silver and gold

A.I. Mares and J.M. van Ruitenbeek
*Kamerlingh Onnes Laboratorium, Universiteit Leiden,
 P.O. Box 9504, 2300 RA Leiden, The Netherlands*
 (Dated: March 23, 2022)

We extend our previous shell effect observation in gold nanowires at room temperature under ultra high vacuum to the other two noble metals: silver and copper. Similar to gold, silver nanowires present two series of exceptionally stable diameters related to electronic and atomic shell filling. This observation is in concordance to what was previously found for alkali metal nanowires. Copper however presents only electronic shell filling. Remarkably we find that shell structure survives under ambient conditions for gold and silver.

PACS numbers: 73.40.Jn, 61.46.+w, 68.65.La

I. INTRODUCTION

Evidence shows that the stability of metallic nanowires is strongly correlated to their electrical properties. Applying a free electron model to a cylindrical nanowire, the electronic free energy as a function of the radius shows an oscillating spectrum with minima that represent stable nanowire configurations due to shell filling [1]. Experimental evidence of shell filling in metallic nanowires was reported for alkali metal nanowires by Yanson *et al.* [2]. Similar to metal clusters [3], alkali metal nanowires present two series of stable diameters, due to electronic and atomic shell filling [4].

In our previous work [5] we reported evidence that shell filling effects are also present in gold nanowires. In this paper we extend the study to the other two monovalent noble metals: silver and copper. The noble metal nanowires are more suitable for applications, being less reactive than the alkali metal nanowires. It would be of great importance to be able to predict and control nanowire stability. Noble metals differ from alkali ones in the shape of Fermi surface (nearly spherical vs almost perfectly spherical) and also in the bulk packing (fcc vs bcc). To some extent the free electron model can be applied also to noble metals nanowires, as was proven successfully for noble metal clusters [3]. We present evidence that, similar to gold, silver and copper nanowires show certain exceptionally stable diameters of the same origin: shell filling. Firstly, we see electronic shell effects in all three metals. Secondly, the atomic shell effect appears only in gold and silver nanowires. Silver however, is exceptional, regarding the more pronounced shell structure as well as the small variation in the peak positions. Remarkably, we find that for gold and silver some of the stable diameters survive even under ambient conditions, which is a big step in the direction of possible applications.

II. EXPERIMENTAL TECHNIQUE

The stability analysis of the noble metal nanowires is done by investigating electrical conductance using

a mechanically controllable break junction (MCBJ) method. A bulk poly-crystalline metal wire is notched circularly and fixed on a substrate. By bending the substrate with a piezoelectric element the wire breaks at the most sensitive point, the notch. By retracting the piezoelement the contact between the two bulk pieces will be remade. Controlling the voltage on the piezoelectric element, one can finely control the dimensions of the contact with atomic resolution. In the process of thinning down, the contact experiences different metastable configurations, depending on the atomic rearrangements in the nanowire and its close vicinity.

Since we search for stable diameters, the atoms need to have sufficient mobility to select the most favorable among all possible metastable configurations. One way to enhance their mobility is by increasing the thermal energy. The optimal temperature is a significant fraction of the melting temperature but one has to take into account that for nanowires the melting temperature is strongly suppressed. For example Hwang *et al.* [6] find in a calculation for copper nanowires of 34 atoms in cross section a melting temperature of 590 K (compared to bulk value 1357 K). On the high end the optimal temperature is limited by the reduced lifetime of the

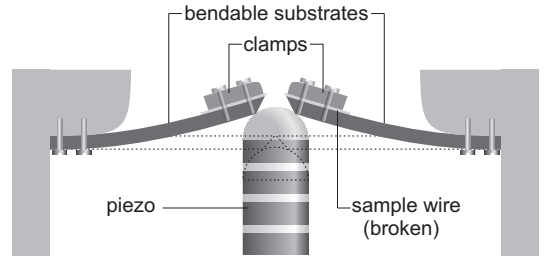


FIG. 1: Schematic view of the MCBJ technique under UHV. The notched sample wire is clamped onto two separate beams and broken by bending the beams. Contact between the fracture surfaces can be finely adjusted by means of the piezoelectric element. The relaxed configuration of the sample is represented by the dotted lines.

metastable states at elevated temperatures. Bürki *et al.* [7] give an estimate of the relevant activation energies, which are more than a factor of two higher for the noble metals as compared to the alkali metals.

We have developed a new MCBJ technique adapted to the use at elevated temperatures in ultra high vacuum (UHV). The bending beam consists of two bendable phosphor bronze substrates where the notched wire is fixed by stainless steel clamps (Fig. 1). The bending beams are mounted on separate stainless steel supports such that the only electrical contact between them is formed by the wire (Fig. 1). The base pressure during measurements is 4×10^{-10} mbar and the temperature range achievable is approximately 70K- 500K. The cooling down is done by thermal contact of the sample substrate with a nitrogen bath. The sample can also be locally heated by radiation from a tungsten filament. The temperature is monitored by a type E thermocouple. We have improved our previous design such that our new sample holder has a tray of six bending beams with a sample mounted on each, that we can independently measure, avoiding in this way to break the vacuum for each new wire.

The conductance is measured at constant bias voltage, recording the current with a current-voltage converter using a digital to analog card of 16 bits resolution. The contact is thinned down starting from about $100 G_0$ in about one second. Here, $G_0 = 2e^2/h$ is the quantum of conductance and $100 G_0$ roughly corresponds to ~ 100 atoms in cross section. Different breaking times in the range of 10 ms to few minutes and different dimensions of the starting contact were tested. A typical conductance trace follows a step like pattern, with plateaus for metastable configurations of the contact and jumps resulting from atomic rearrangements in the vicinity of the contact. In order to find only the preferred diameters from all metastable configurations, we use a statistical analysis, by adding many conductance traces in a histogram. The conductance scale is divided into about 600 bins, and a histogram is build from a few thousands of scans. A peak in the histogram corresponds to a preferred, reproducible configuration of the contact.

III. RESULTS

A. Electronic shell effects

Fig. 2 presents a conductance histogram recorded at room temperature under UHV (UHV-RT) using a bias voltage of 100 mV. The histogram reproduces our previously reported result [5]. One can see a sequence of distinct peaks at certain conductance values. In the low conductance range peaks are situated close to 1, 2, 3 G_0 the conductance for 1, 2, 3 atoms in cross section, as reported previously for gold atomic contacts [8, 9]. We see that these peaks have a relatively low amplitude, the

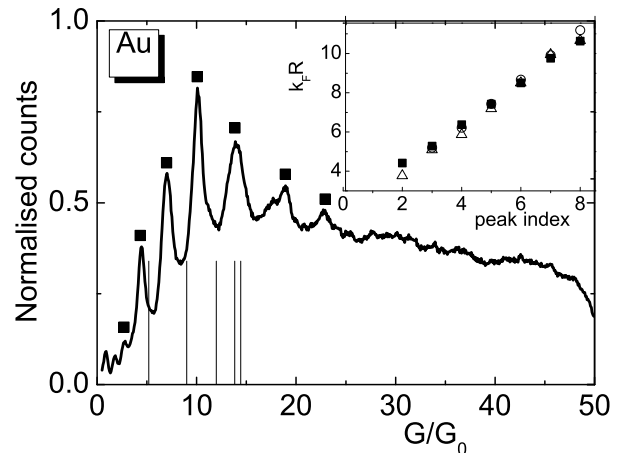


FIG. 2: Conductance histogram for gold at room temperature under UHV constructed from 5000 individual consecutive traces, using a bin size of $0.1 G_0$ and a bias voltage of 100 mV, giving evidence of electronic shell filling. Peak positions are indicated by squares. By bars we plot the calculated conductance for helical nanowires [10]. The inset shows the peak positions, converted to $k_F R$ with the help of Eq. (1), as a function of peak index (filled squares), magic radii for gold clusters (circles) [11], and predictions of the minima of the electronic energy calculation (triangles) taken from [12]. The experimentally observed periodicity of the peaks is $\Delta k_F R = 1.06 \pm 0.01$.

maximum being at the peak of $10 G_0$.

For the regime of thick nanowires the conductance is related to the nanowire radius by a semi-classical formula for a ballistic nanowire with circular cross section:

$$G = gG_0 \cong G_0 \left[\left(\frac{k_F R}{2} \right)^2 - \frac{k_F R}{2} + \frac{1}{6} + \dots \right], \quad (1)$$

with $k_F R$ the Fermi wave vector, g the reduced conductance and R the radius of the nanowire [13], [14]. When we plot the peak positions in units $k_F R$ as function of peak index we get a linear dependence, illustrated in the inset of Fig. 2 with a slope $\Delta k_F R = 1.06 \pm 0.01$, similar to the one obtained for alkali metals. This is an indication that the peaks in the conductance histogram are due to electronic shell filling: the nanowire chooses such diameters that give minima in the electronic free energy.

We now find similar periodic patterns for silver and copper nanowires as one can see in the histograms of Fig. 3. The periodicity of the peaks is similar to gold. Thus for silver and copper the slope is $\Delta k_F R = 0.98 \pm 0.01$. The maximum spectrum amplitude for silver is found at about $15 G_0$, while for gold and copper it varies between different measurements on values 7, 10, 12 for gold and 10, 14, 18 for copper.

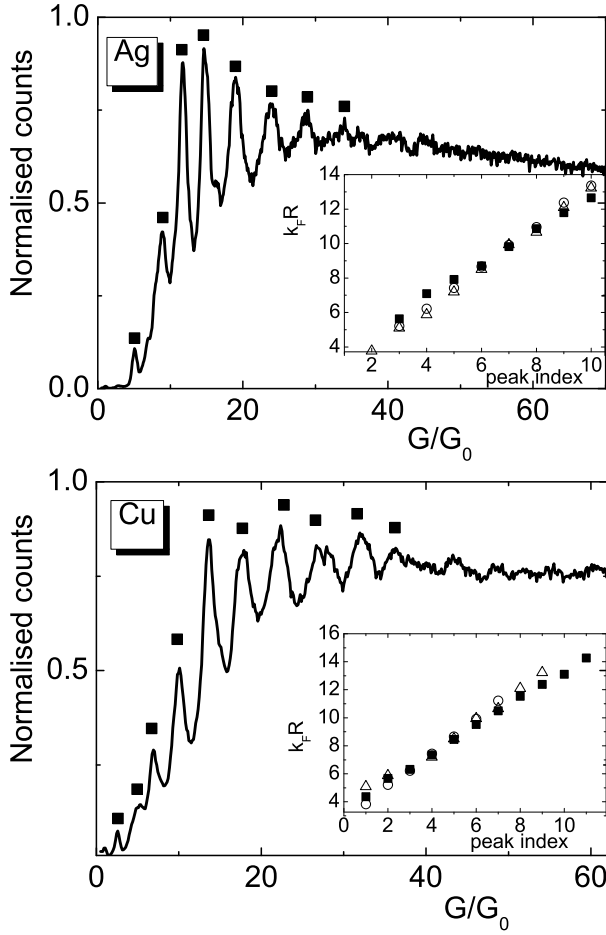


FIG. 3: Conductance histogram for silver (top) and copper (bottom) at room temperature, giving evidence of electronic shell filling. The silver histogram is constructed from 10000 individual consecutive traces, using a bin-size of $0.1 G_0$, while for copper 20000 individual consecutive traces were included and a bin-size of $0.14 G_0$ was used. In each case the bias voltage was 100 mV. The insets show the peak positions, converted to $k_F R$, as a function of peak index (filled squares). The slope is $\Delta k_F R = 0.98 \pm 0.01$, both for silver and copper. Magic radii for silver and copper clusters [11] and theoretical predictions for stable diameters in nanowires [12] are shown for comparison (circles and triangles, respectively).

B. Atomic shell effects

Sometimes a new series of peaks appears in the histogram as we can see in Fig. 4 (top), that was reported in our previous work [5] recorded for gold in UHV-RT. This is related to a geometrical effect also present in clusters, namely, atomic shell filling. Certain nanowires are more stable when they adopt a crystalline order with smooth facets such as to obey minima of surface energy. This effect is expected to appear at larger diameters than electronic shell filling. Silver nanowires present this new series of stable diameters even more pronounced than

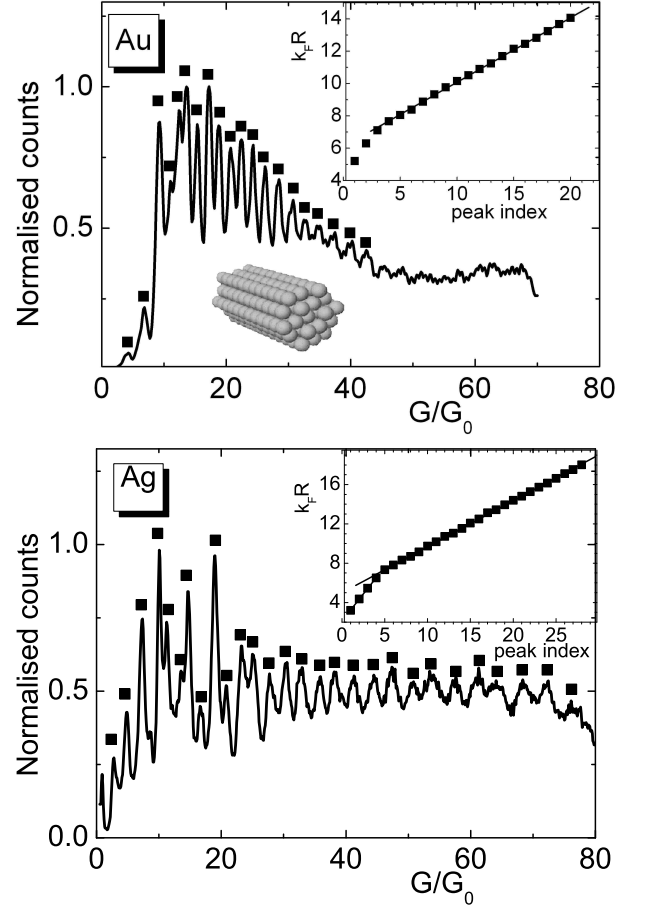


FIG. 4: Conductance histogram for Au (top) and silver (bottom) obtained from 3000 and 4500 individual conductance traces, respectively, recorded under UHV-RT, giving evidence of electronic and atomic shell effects. The bias voltage was 150 mV for gold and 100 mV for the silver measurements. We observe a cross over from electronic to atomic shell structure at $G \sim 10 G_0$. Peak positions as function of peak index (top insets) exhibit a linear dependence as expected for atomic shell effect with slopes of $\Delta k_F R = 0.400 \pm 0.002$ and $\Delta k_F R = 0.460 \pm 0.001$ for gold and silver, respectively. The lower inset in the top panel shows a sketch of a nanowire along the $[110]$ axis with hexagonal cross section with four (111) facets and two larger (100) ones.

gold does, with peaks up to conductance values of $80 G_0$ (see Fig. 4). However, for copper we have not observed distinct atomic shell effect peaks.

The crossover between electronic and atomic shell effects is in most of the cases around $10 G_0$ for gold, and at about $15 G_0$ for silver but it can vary around this value between different measurements. This variation can be due to local crystalline orientation, a parameter that we cannot control during measurements. The crossover value is in some histograms hard to determine since besides the consecutive series of peaks having atomic shell effect periodicity electronic shell effect peaks appear to be su-

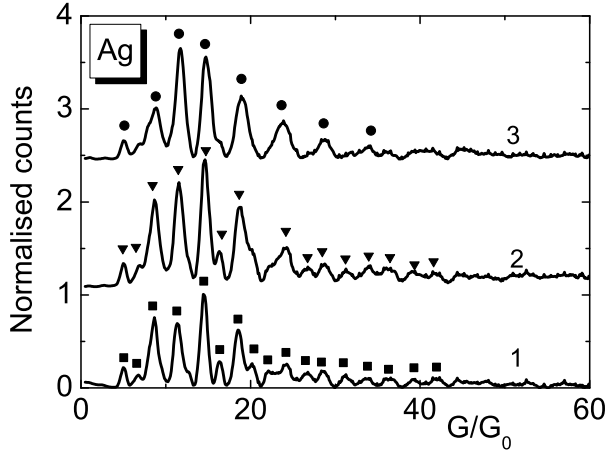


FIG. 5: Evolution of Ag conductance histograms obtained in UHV-RT recorded at a bias voltage of 100 mV during the same measurement, containing 5000 traces (1), 8000 traces (2), and 20000 traces (3). Histogram (3) includes the traces of histograms (2) and (1). From all three curves a smooth background was subtracted. In curves (1) and (2) the peaks obey atomic shell effect period, while in curve (3) a transition to electronic shell effect period occurs.

perimposed.

We observe that during a particular measurement, after repeated cycles of making and breaking the contact, an evolution from atomic shell effect to electronic shell effect appears, as one can see in Fig. 5. Curves 1, 2, 3 are histograms recorded during the same measurement containing 5000, 8000, and 20000 consecutive scans. A smooth positive background was subtracted from the histograms for better clarity. Firstly we can see that some peaks having atomic shell effect periodicity in histogram 1 gradually decrease their weight in histogram 2 until they disappear in histogram 3 (peaks at $G \sim 7, 16, 20, 22, 26$, and all the peaks above this value). Secondly we see that in histogram 3 the peaks vanish above $30 G_0$, while in histograms 1, 2 they are visible up to about $40 G_0$. Finally in the histogram 3 we get peaks that have electronic shell effect periodicity. This transition from atomic to electronic shell effect was reported previously also for alkali metals [15], and can be due to an increase in mobility of the atoms during repeated cycles of elongation/compression of the nanowire, that can damage the faceting. Another possible reason may be that during repeated indentation the crystalline orientation of the nanowire or of the connecting electrodes changes, not being favorable anymore for faceting.

C. Experiments under ambient conditions

Fig. 6 (top) shows a conductance histogram for gold recorded at room temperature under ambient conditions. One can clearly distinguish peaks up to about $22 G_0$,

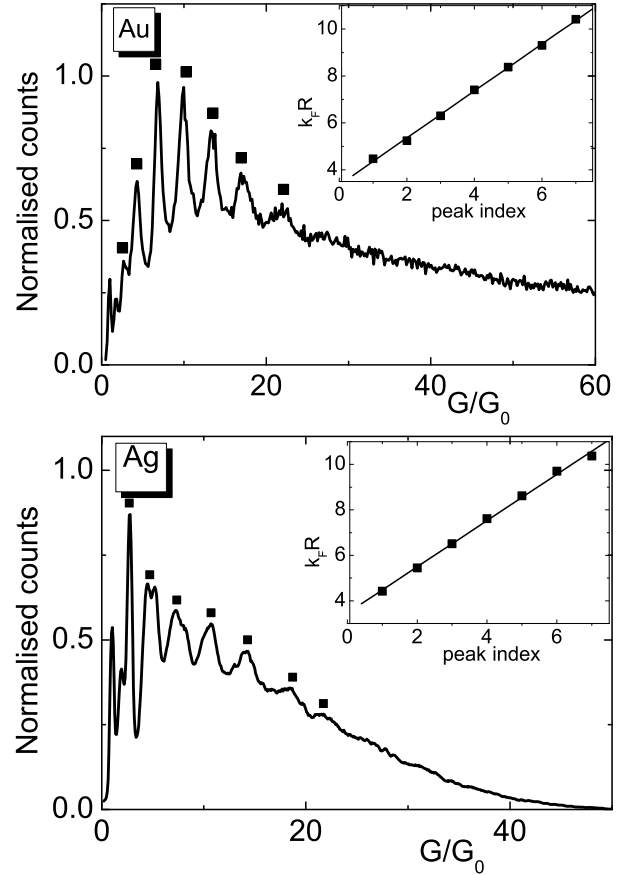


FIG. 6: Conductance histograms for gold (top) and silver (bottom) at room temperature under ambient conditions, constructed from 2000 and 10000 individual consecutive traces, respectively, giving evidence of electronic shell filling. The bin size was $0.13 G_0$ (gold) and $0.08 G_0$ (silver) and the bias voltage of 100 mV (gold) and 20 mV (silver). The insets show the peak positions, converted to $k_F R$, as a function of peak index with a slope $\Delta k_F R = 1.00 \pm 0.01$ (gold) and $\Delta k_F R = 1.06 \pm 0.02$ (silver).

with a periodicity $\Delta k_F R = 1.00 \pm 0.01$, very close to the value obtained in UHV. The peak positions are close to the ones obtained in UHV, although some of them may be shifted somewhat to lower values. Similarly, a silver conductance histogram in air shows electronic shell effect periodicity $\Delta k_F R = 1.06 \pm 0.02$ (Fig. 6, bottom). This brings evidence that, remarkably, shell structure survives even under ambient conditions in silver and gold. The relative intensity of the peaks is different from those under UHV. The maximum amplitude is shifted to lower conductance values with respect to UHV. Moreover the peak at about $1 G_0$, commonly attributed to a single-atom contact [16] has a much higher amplitude than under UHV. It has been shown by Hansen *et al.* [17] that a one-atom contact is hardly stable under UHV-RT, due to the high mobility of the atoms. However, under ambient conditions adsorbates decrease the atom mobility result-

ing in an enhanced stability of small contacts. This may explain the experiments on gold atomic contacts at RT in air [8]. In our conductance histograms we see that only the electronic shell effect survives in air. This is not unexpected since the atomic shell effect is a surface effect, therefore adsorbed species modify the surface energy and are expected to damage the faceting.

Copper does not show shell effect peaks in air. The dominant feature is a broad peak close to $1 G_0$, as previously reported [18]. Since copper is known to be the most reactive of the three noble metals, the absence of shell structure can be caused by fast oxidation of the contact.

IV. DISCUSSION

A. Comparison with low temperature histograms

Conductance histograms for gold at low temperatures reported in the literature typically show only the range of low conductances that is dominated by a peak near $1 G_0$, attributed to a one atom contact, see e.g., results on gold at liquid helium temperatures [9]. Peaks can be distinguished only up to $3G_0$ followed by a flat tail. For copper and silver conductance histograms recorded at helium temperature are similar to gold having a dominant peak at or just below $1G_0$, followed by two additional peaks of lower intensity [19]. There is a major difference in the origin of the low temperature peaks compared to our UHV-RT histograms. At low temperature the atoms are frozen in configurations that have a certain conductance value. In UHV-RT measurements atomic mobility plays an important role and the nanowire can self-organize such to find the most stable configuration. Therefore, the peaks in our data reflect preferred stable diameters, and not preferred conductance like in the case of low temperature histograms.

B. Comparison between the three different noble metals

In Fig. 7 we plot the averaged values of the peak positions in histograms showing electronic shell structure recorded from different independent measurements for gold, silver and copper. We observe that the peak positions are very close to each other for the three metals. There are variations for the gold peaks indexed 6 and 9. It is possible that one peak is missing in the histograms because of the supershell modulation of the peak amplitudes, [20], as it will be explained later. The standard deviation is quite low, showing that the stable diameters can be reproduced very well in different measurements. We believe that the small shifts that are observed come from variations in the conductance due to back-scattering on defects near the contacts.

C. Electronic shell effect theory

The periodic pattern present in our histograms in Figs. 2 and 3 is due to minima in the electronic free energy of the nanowire as function of elongation. We compare our peak positions with the theoretically predicted stable diameters reported by Ogando *et al.* [12]. The theoretical model used is called stabilized jellium model and considers the nanowire as an infinitely long cylinder taking into account the average valence electron density of the metal. With this assumption the energy oscillations as function of radius are obtained, having minima due to shell filling. These minima agree well with the experimentally obtained stable diameters for the three metals in question, as we can see in the insets of Figs. 2 and 3 (triangles) and in Fig. 7 (crosses).

The physical mechanism leading the magic series of diameters is best illustrated using a semiclassical approach. The electron moves classically in the circular cross section of the wire. The stable diameters are determined by closed orbits inside the cylindrical walls of the wire. The orbits that proved to have the most significant contribution for alkali nanowires are the diametric, triangular and square orbits [9], [20]. The oscillating frequencies that result from these orbits are $1/\Delta k_F R = 0.64$ for diametric orbit and $1/\Delta k_F R = 0.83$, $1/\Delta k_F R = 0.90$ for triangular and square orbits. A beating effect known as supershell effect appears due to the superposition of the diametric orbit with the higher frequency orbits (triangular and square). In order to separate the oscillating frequencies in the experimental histograms we perform a Fourier transform. Since we are interested in only the oscillatory part of the spectra in Figs. 2 and 3 we subtract a smooth background. The Fourier transform for Au (Fig.

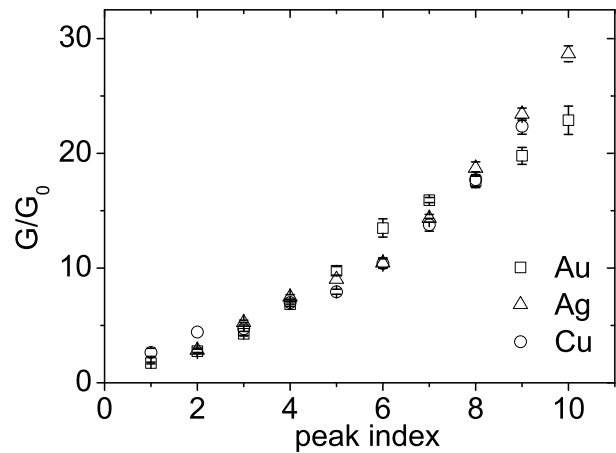


FIG. 7: Averaged peak positions and their standard deviations obtained from conductance histograms of independent measurements for Ag (11 measurements; squares), Cu (12 measurements; circles), and Au (5 measurements; triangles). Results of the stabilized jellium model considering a circular cross section are also included (crosses) [12].

8, top) shows a broad peak centered at a frequency of $1/\Delta k_F R = 0.92$. This value is somewhat higher than what is expected from the superposition of the triangular and square orbits. This deviation can be seen as due to conductance lowering due to backscattering on defects in or near the nanowire. This correction seems to be contact size dependent, as seen by the fact that the conductance is lowered, but the calculated radii of the contact are still linear with peak index, as seen in the insets of Figs. 2 and 3. Indeed the slope is somewhat lower than what obtained from stabilized free electron model calculation [12] $\Delta k_F R = 1.19 \pm 0.02$, and also by comparison to the results on potassium and sodium nanowires [9]. However deviations of the same order have been observed for lithium nanowires attributed to the same defect scattering effect [9]. In the case of silver and copper the dominant peak in the Fourier transform is centered on even higher frequencies $1/\Delta k_F R = 0.97$ and $1/\Delta k_F R = 0.99$. The contribution of the diametric orbit seems to be less important in the spectra for the noble metal nanowires as compared to the alkali metals. We might identify a broad peak around $1/\Delta k_F R = 0.68$ for silver and copper as being due to the diametric orbit. Again, the fre-

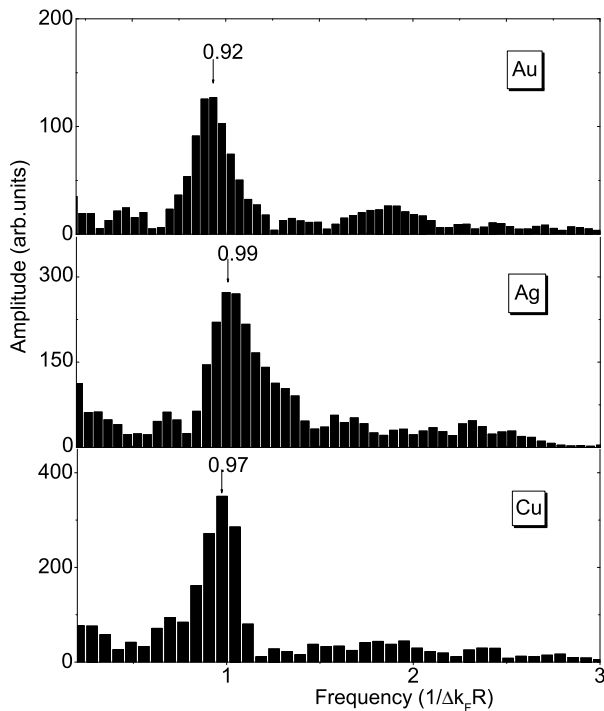


FIG. 8: Fourier transform of the conductance histograms showing electronic shell effect for gold, silver and copper. The Fourier spectra presents one main frequency that can be attributed to a superposition of triangular and square orbit. The diametric orbit expected at the frequency of $1/\Delta k_F R = 0.64$ might be identified as the peak situated at about $1/\Delta k_F R = 0.68$ for silver and copper, being less pronounced for the latter. For gold there is no clear peak around this value.

quency is somewhat higher than predicted by the semiclassical model for a clean wire. For gold there is no clear contribution of the diametric orbit. The selective suppression of the diametric orbit may be explained in terms of backscattering on surface roughness. For the circular orbit the incoming electron wave is perpendicular to the surface being therefore more probable to be diffusely scattered than in the case of grazing incidence orbits. Another reason can be the low resolution we have in the fourier transform because of the limited number of peaks.

By applying a free electron model to noble metals one ignores the non-spherical shape of their Fermi surfaces. The main sheets of the bulk Fermi surface are connected by necks at Brillouin zone boundaries along the [111] orientation. However, the contribution of the necks to the oscillations in the density of states is expected to be small since their wavelength is about six times larger than the main Fermi wavelength, for gold and copper. Filling of the states in the neck will have a period six times larger than the one resulting from the states in the belly. The silver Fermi surface has even smaller deviations, resulting in a wavelength and a period of resulting oscillations of density of states eight times higher than those in the belly. Moreover the contribution of the states of the necks to the total density of states is relatively small. Therefore, in a good approximation Au, Ag, and Cu may be considered free electron metals. Our assumption is supported by electronic structure calculations for the quantum modes in nanowires of Na and Cu [21].

D. Comparison to magic numbers of noble metal clusters

We compare also the values for the preferred nanowire diameters with the magic radii in clusters (circle symbols in Figs. 2 3, obtained from the number of atoms in a cluster, N , as $k_F R = 1.919 N^{1/3}$ [3]). We see that the agreement is very good. This is at first sight unexpected due to the difference of symmetry, that is spherical in the case of clusters and cylindrical for nanowires. However, we first note that the gross features of distribution of zeros for spherical and cylindrical Bessel functions are nearly identical for not too large diameters. The difference between cylindrical and spherical geometries is expressed mostly in the relative weight of the various semiclassical orbits. For nanowires the diametric orbit is expected to have a strong contribution in the oscillation spectrum while for clusters it is negligible. Since we have very little influence of the diametric orbit, possibly as a result of surface roughness, we obtain about the same oscillation period as for noble metal clusters.

E. Atomic faceting

At larger diameters, the surface energy becomes more important than the free energy. The oscillation amplitudes of the electronic free energy have a $1/R$ dependence [22] while the ones for surface energy are roughly constant. A crossover between the two is experimentally observed by the change in the oscillation period. We propose a model for nanowire faceting starting from the crystalline order that we have in bulk: fcc for all three noble metals. We assume that the nanowires form along the [110] axis having a hexagonal cross section with four (111) facets and two larger (100) ones (inset of Fig. 4). The filling of each individual facet will give a stable diameter. There has been another proposed cross section of the nanowire with octagonal symmetry [23]. We have chosen the hexagonal cross section along the [110] orientation supported by high resolution transmission electron microscopy (HRTEM) observations [24], [25]. These experiments provide evidence that the bulk crystalline order survives in gold and copper atomic contacts. The atomic arrangement of the nanowires obtained by means of the Wulff construction reveal that the growth occurs preferentially along the crystalline directions [110], [111], and [100], with the first one being more favorable for growing long nanowires. Our model is further supported by Monte Carlo simulations that confirm that for the process of thinning down of a nanowire the [110] direction is a preferred orientation for forming long and stable nanowires with a faceted structure [26]. The expected periodicity of stable diameters is $\Delta k_F R = 0.476$. This value is very close to the experimentally observed periodicity for gold $\Delta k_F R = 0.40$ and even closer for silver $\Delta k_F R = 0.46$. Silver also has the largest number of atomic shell effect peaks, as one can see in Fig. 4.

Previous results on copper nanowires in UHV-RT have been reported by combining HRTEM and MCBJ [25]. From independent imaging and conductance measurements of copper nanowires Gonzales *et al.* suggest that a stable pentagonal configuration occurs having a conductance of $4.5 G_0$.

In most of the cases (7 out of 10 measurements) our conductance histograms for copper show a peak at $5 G_0$, and very rarely at lower values between $4 G_0$ and $4.5 G_0$. Similarly for silver the peak position is close to $5 G_0$. However for gold we reproducibly see a distinct peak close to $4 G_0$. This peak was tentatively attributed to an quadrupolar distorted nanowire that gold may have preference to form [27]. Such distortions would be most likely when the surface tension is low. The surface tension for gold lies in between that for Cu and Ag, which seems to rule out this interpretation. We propose that the d-bonding character for gold that also gives rise to the formation of atomic chains [28] may play a role for the smallest contacts.

Kondo *et al.* reported the formation and imaging of suspended multi-shell helical gold nanowires with diameters ranging from 0.6 nm and length of 6 nm [29]. Such anomalous atomic arrangements in nanowires, referred to as ‘weird wires’, had been predicted from model calculations by Güleren *et al.* [30]. Recently the conductance of these structures was calculated by first principle methods [10]. We compare in Fig. 2 the calculated values of the conductance for the multi-shell helical wires with our peak positions. One can observe that the period for the first few peaks is close to the period of the calculated helical nanowire conductances, although their values do not fully coincide. However, at higher conductances the bars start to get closer together in contrast to the peaks in the histogram. We do not exclude the formation of helical nanowires, but we believe the peaks in the histogram are due to shell effect considering the agreement with the theoretically predicted period [12]. The reason why helical wires form in the experiment by Kondo *et al.* and not in ours is likely to be attributed to the different experimental methods for forming the nanowires.

V. CONCLUSION

We have evidence that electronic shell filling influences the formation and stability of all three noble metal nanowires: gold, silver and copper. At larger diameters the atomic shell effect is dominant and appears in gold and silver but was not observed in copper. We observe that the shell structure is the most pronounced in silver nanowires. Regarding the electronic shell structure the Fourier spectrum reveals that the main contribution comes from the superposition of triangular and square orbits. Free electron model predictions of stable radii due to the shell effect agree well with our results. Predicted values of conductance for gold elliptically distorted nanowires agree with the experimental peaks. Our stable diameters are in good agreement with the magic diameters of noble metal clusters. Together with the results for alkali metals [2, 4, 9, 15], we thus conclude that shell effects are generally observed for monovalent metals. The effect is sufficiently robust that it can be observed under ambient conditions for gold and silver.

Acknowledgments

We thank C. A. Stafford for valuable discussions and R. van Egmond for technical support. This work is part of the research program of the “Stichting FOM,” and was further supported by the European Commission TMR Network program DIENOW.

-
- [1] C. A. Stafford, D. Baeriswyl, and J. Bürki, Phys. Rev. Lett. **79**, 2863 (1997).
 - [2] A. I. Yanson, I. K. Yanson, and J. M. van Ruitenbeek, Nature **400**, 144 (1999).
 - [3] W. A. de Heer, Rev. Mod. Phys. **65**, 611 (1993).
 - [4] A. I. Yanson, I. K. Yanson, and J. M. van Ruitenbeek, Phys. Rev. Lett. **87**, 216805 (2001).
 - [5] A. I. Mares, A. F. Otte, L. G. Soukiassian, R. H. M. Smit, and J. M. van Ruitenbeek, Phys. Rev. B **70**, 073401 (2004).
 - [6] H. J. Hwang and J. W. Kang, Surf. Sci. **532-535**, 536 (2003).
 - [7] J. Bürki, C. A. Stafford, and D. L. Stein (2005), preprint, cond-mat/0505221.
 - [8] J. L. Costa-Krämer, Phys. Rev. B **55**, R4875 (1997).
 - [9] A. I. Yanson, Ph.D. thesis, Universiteit Leiden, The Netherlands (2001).
 - [10] T. Ono and K. Hirose, Phys. Rev. Lett. **94**, 206806 (2005).
 - [11] I. Katakuse, T. Ichihara, Y. Fujita, T. Sakurai, and H. Matsuda, Int. J. Mass Spectrom. Ion Processes **67**, 229 (1985).
 - [12] E. Ogando, N. Zabala, and M. Puska, Nanotechnology **13**, 363 (2002).
 - [13] J. A. Torres, J. I. Pascual, and J. J. Sáenz, Phys. Rev. B **49**, 16581 (1994).
 - [14] C. Höppler and W. Zwerger, Phys. Rev. Lett. **80**, 1792 (1998).
 - [15] A. I. Yanson, I. K. Yanson, and J. M. van Ruitenbeek, Low Temp. Phys. **27**, 1092 (2001).
 - [16] E. Scheer, N. Agraït, J. C. Cuevas, A. Levy Yeyati, B. Ludoph, A. Martín-Rodero, G. Rubio Bollinger, J. M. van Ruitenbeek, and C. Urbina, Nature **394**, 154 (1998).
 - [17] K. Hansen, S. K. Nielsen, M. Brandbyge, E. Lægsgaard, I. Stensgaard, and F. Besenbacher, Appl. Phys. Lett. **77**, 708 (2000).
 - [18] K. Hansen, E. Laegsgaard, I. Stensgaard, and F. Besenbacher, Phys. Rev. B **56**, 2208 (1997).
 - [19] J. M. Krams, C. J. Muller, I. K. Yanson, T. C. M. Goovaert, R. Hesper, and J. M. van Ruitenbeek, Phys. Rev. B **48**, 14721 (1993).
 - [20] A. I. Yanson, I. K. Yanson, and J. M. van Ruitenbeek, Phys. Rev. Lett. **84**, 5832 (2000).
 - [21] J. Opitz, P. Zahn, and I. Mertig, Phys. Rev. B **66**, 245417 (2002).
 - [22] C. Yannouleas, E. N. Bogachek, and U. Landman, Phys. Rev. B **57**, 4872 (1998).
 - [23] E. Medina, M. Díaz, N. León, C. Guerrero, A. Hasmy, P. A. Serena, and J. L. Costa-Krämer, Phys. Rev. Lett. **93**, 186403 (2004).
 - [24] V. Rodrigues, T. Fuhrer, and D. Ugarte, Phys. Rev. Lett. **85**, 4124 (2000).
 - [25] J. C. Gonzalez, V. Rodrigues, J. Bettini, L. G. C. Rego, A. R. Rocha, P. Z. Coura, S. O. Dantas, F. Sato, D. S. Galvao, and D. Ugarte, Phys. Rev. Lett. **93**, 126103 (2004).
 - [26] E. A. Jagla and E. Tosatti, Phys. Rev. B **64**, 205412 (2001).
 - [27] D. F. Urban, J. Bürki, C.-H. Zhang, C. A. Stafford, and H. Grabert, Phys. Rev. Lett. **93**, 186403 (2004).
 - [28] R. H. M. Smit, C. Untiedt, A. I. Yanson, and J. M. van Ruitenbeek, Phys. Rev. Lett. **87**, 266102 (2001).
 - [29] Y. Kondo and K. Takayanagi, Science **289**, 606 (2000).
 - [30] O. Gülseren, F. Ercolessi, and E. Tosatti, Phys. Rev. Lett. **80**, 3775 (1998).